Neuron, Vol. 42, 947–959, June 24, 2004, Copyright ©2004 by Cell Press

Chromatin Acetylation, Memory, and LTP Are Impaired in CBP$^{+/-}$ Mice: A Model for the Cognitive Deficit in Rubinstein-Taybi Syndrome and Its Amelioration

Juan M. Alarcón,[1,4] Gaël Malleret,[1,4] Khalid Touzani,[1] Svetlana Vronskaya,[1] Shunsuke Ishii,[3] Eric R. Kandel,[1,2,*] and Angel Barco[1]

[1]Center for Neurobiology and Behavior
College of Physicians and Surgeons
[2]Howard Hughes Medical Institute
Columbia University
1051 Riverside Drive
New York, New York 10032
[3]Laboratory of Molecular Genetics
RIKEN Tsukuba Institute
Tsukuba, Ibaraki 305-0074
Japan

Summary

We studied a mouse model of the haploinsufficiency form of Rubinstein-Taybi syndrome (RTS), an inheritable disorder caused by mutations in the gene encoding the CREB binding protein (CBP) and characterized by mental retardation and skeletal abnormalities. In these mice, chromatin acetylation, some forms of long-term memory, and the late phase of hippocampal long-term potentiation (L-LTP) were impaired. We ameliorated the L-LTP deficit in two ways: (1) by enhancing the expression of CREB-dependent genes, and (2) by inhibiting histone deacetyltransferase activity (HDAC), the molecular counterpart of the histone acetylation function of CBP. Inhibition of HDAC also reversed the memory defect observed in fear conditioning. These findings suggest that some of the cognitive and physiological deficits observed on RTS are not simply due to the reduction of CBP during development but may also result from the continued requirement throughout life for both the CREB co-activation and the histone acetylation function of CBP.

Introduction

Mutations in the gene encoding for the cAMP-responsive element binding protein (CREB) binding protein (CBP) result in Rubinstein-Taybi syndrome (RTS), a rare condition that occurs in 1/125,000 births and is characterized by mental retardation and skeletal abnormalities (Petrij et al., 1995). Although CBP was originally identified as a co-activator of CREB (Chrivia et al., 1993), it was later found to be required as a cofactor for many transcription factors (Chan and La Thangue, 2001). CBP also plays a double role in transcription activation: (1) it acts as a scaffold protein interacting directly with diverse transcription factors and with components of the RNA polymerase II (Pol II) complex, thereby recruiting this complex to the promoter, and (2) it acts as a histone acetyltransferase that contributes to transcription activation by acetylating specific lysine residues in histones of nucleosomes, thereby disrupting repressive chromatin structure (Chan and La Thangue, 2001). Loss of function of CBP may therefore interfere with the transcriptional activation of target genes in two ways: by preventing recruitment to the promoter of the basal transcription machinery and by blocking chromatin remodeling.

CREB occupies a prominent position among the transcription factors that regulate the changes in gene expression required for the acquisition and storage of new memories, as evident in a variety of experimental systems ranging from mollusks to mammals (Kandel, 2001; Lonze and Ginty, 2002). CREB phosphorylation enables interaction with CBP and links several kinase pathways, driven by neuronal activity, to transcriptional activation of specific promoters. Recent findings indicate that the transactivation potential of CREB might be directly modulated through acetylation of specific lysine residues by CBP (Lu et al., 2003). Other transcription factors known to be activated during activity-dependent neuronal gene expression, such as c-Fos (Janknecht and Nordheim, 1996), c-Jun (Bannister et al., 1995), or NF-κβ (Gerritsen et al., 1997; Perkins et al., 1997), also interact with CBP, although their specific roles in synaptic plasticity and memory are more poorly understood (Herdegen and Leah, 1998). In addition, CBP is itself regulated by activity-dependent phosphorylation (Hu et al., 1999; Impey et al., 2002).

Despite the fact that CBP is the common target in patients with RTS, there is a wide variation in the severity of mental retardation and other clinical features. The intelligence level of affected individuals is usually low, with an average IQ of 51, but some patients have much higher scores. These differences could be due to the heterogeneity of chromosomal rearrangements in the *cbp* gene observed in RTS patients and to the existence of two different mechanisms for transcriptional dysfunction: (1) haploinsufficiency and (2) dominant-negative action of truncated CBP protein (Coupry et al., 2002; Petrij et al., 1995, 2000). Mouse models corresponding to each one of these molecular mechanisms have now been generated (Oike et al., 1999a; Tanaka et al., 1997), and their comparison is likely to be useful not only for elucidating the etiology of this syndrome but also its varied expression.

The first mouse model for RTS, a conventional knockout of the *cbp* gene, was generated by Tanaka and colleagues. Mice homozygous for this mutation die early during development (Tanaka et al., 1997, 2000) and heterozygous mutants exhibit phenotypes resembling some of the clinical features of RTS, such as growth retardation and various skeletal abnormalities. A second model for RTS, an insertional mutation into the *cbp* gene leading to the expression of a truncated CBP protein, was generated later by Oike and colleagues (Oike et al., 1999a). Embryos homozygous for this mutation also died early in utero, while heterozygous mice showed more severe clinical features of RTS than those in the null allele RTS model, indicating a possible dominant-negative effect in the etiology of the syndrome (Oike et

*Correspondence: erk5@columbia.edu
[4]These authors contributed equally to this work.

al., 1999a, 1999b; Yamauchi et al., 2002). This interpretation is supported by the finding that truncated CBP protein interferes with transcriptional activation mediated by full-length CBP (Parker et al., 1996). However, this dominant mutation is found only in a low percentage of RTS individuals (about 10%; Perkins et al., 1997; Petrij et al., 2000); therefore, the null allele heterozygous mutant mice (*cbp*$^{+/-}$) appear to be a more realistic model for the major form of RTS.

Earlier behavioral studies on mouse models for RTS have focused on the dominant-negative action of the truncated CBP protein. Using step-through passive avoidance and fear conditioning tasks, Oike et al. first found that mice expressing a truncated CBP were deficient in long-term memory (LTM) but not in short-term memory (STM) (Oike et al., 1999a). More recently, Bourtchouladze et al. confirmed this deficit in long-term memory using an object recognition task (Bourtchouladze et al., 2003). However, the severe phenotype of truncated CBP mutants, including cardiac anomalies and hypolocomotion (Oike et al., 1999a, 1999b), may confound the interpretation of behavioral experiments. Thus, despite the crucial role in memory storage suggested by these preliminary studies of CBP, no neurological or behavioral studies have been carried out in the null allele mouse model for RTS. Moreover, there has been no previous report of electrophysiological deficits in any of the CBP mutants.

To address these issues, we extended the characterization of CBP mutant mice in four ways. First, we confirmed the existence of memory deficits in the null allele mouse model for the haploinsufficiency form of RTS, indicating that a haploinsufficiency mechanism is sufficient to explain the deficits in LTM in the most prevalent form of the disorder. Second, we described the LTP phenotype in a mouse model of RTS. We found that these mice show a specific defect in the late phase of long-term potentiation (L-LTP) that could account for the deficits in long-term memory. This deficit is quite specific; we observed no alteration in E-LTP or in basal synaptic transmission. Third, we found that bulk histone H2B acetylation was reduced in these mutant mice, indicating that chromatin alteration may underlie these defects. Fourth, our results indicate that the reduced L-LTP observed in *cbp*$^{+/-}$ mice can be significantly alleviated by genetic or pharmacological compensation for CBP dysfunction, suggesting that these deficits may be due to a continuous requirement for CBP throughout life and not the consequence of altered brain development leading to permanent anatomical abnormalities. Finally, we describe an enhancement of LTP by an inhibitor of histone deacetylases, a finding that supports a role for chromatin remodeling in long-term synaptic plasticity of the mammalian brain.

Results

Hippocampal Neurons of *cbp* Heterozygous Mice Have a Reduced Level of CBP

In spite of mild skeletal abnormalities in the skull of *cbp*$^{+/-}$ mutant mice (Tanaka et al., 1997) such as enlarged fontanels that slightly change the shape of their heads (Figure 1A, left), these animals do not show any obvious abnormalities in brain anatomy. Nissl staining and immunohistochemistry of brain sections using a variety of neuronal markers (NeuN, calbinding, PSD95, synaptophysin) did not reveal any difference between *cbp*$^{+/-}$ heterozygous and wild-type controls (Figure 1A and data not shown). However, the comparison of hippocampal extracts by Western blotting using CBP-specific antibodies revealed that *cbp*$^{+/-}$ mutants expressed half the wild-type level of CBP (Figures 1B and 1C, $p = 0.009$).

cbp$^{+/-}$ Heterozygous Mice Show Normal Levels of Activity, Motivation, Anxiety, and Working Memory

Behavioral studies on mice carrying a truncated form of CBP have revealed defects in long-term memory as tested in passive avoidance tasks (Oike et al., 1999a) and more recently in an object recognition task (Bourtchouladze et al., 2003). Truncated CBP has a dominant-negative effect on normal CBP and results in a more severe phenotype than is evident in mutants that have a null CBP allele (Tanaka et al., 2000). This phenotype includes reduced locomotive activity (observed in 100% of the mice; Oike et al., 1999a), which could well alter the mouse performance in behavioral test of memory. We therefore investigated the behavioral phenotype of the mouse model for the most common cases of RTS, the *cbp* null allele heterozygous mutant (*cbp*$^{+/-}$). We carried out a comprehensive behavioral analysis of *cbp*$^{+/-}$ heterozygous mice to assess various aspects of brain function, including motor abilities, emotional behavior, learning, and memory.

We first examined *cbp*$^{+/-}$ mice in an open field, a test for anxiety and basic locomotor behavior. Mutant mice showed normal exploratory activity, as assayed by ambulatory time and vertical activity (Figures 2A and 2B and results not shown). We also found no differences between mutant mice and their wild-type siblings in the time spent in the center of the arena, a common measure of anxiety (Figure 2C). We next studied these mice in the elevated plus maze, a task where mice face a conflict between their tendency to explore new environments and their innate aversion to open, brightly lit spaces. Both wild-type and mutant mice showed a similar percentage of open arm entries in the elevated plus maze and both spent a similar amount of time in the open arm (Figure 2D and result not shown). In agreement with our observations in the open field, these parameters indicated normal levels of anxiety and motivation in these mutant mice. We also found no differences between the two genotypes in prepulse inhibition, a test of sensorimotor gating processes (Figure 2E). We did find, however, a significant deficit in the performance of *cbp*$^{+/-}$ mice in an accelerated paradigm for the rotarod task (Figure 2F), a test of motor learning. The deficit in this task may be the result of abnormal motor learning or a direct consequence of the abnormal skeletal patterning and joints of these mice (Tanaka et al., 1997). Humans with RTS, notably, also experience difficulty executing locomotor skill (Gotts and Liemohn, 1977).

Finally, we assayed the performance of *cbp*$^{+/-}$ mice in a spatial working memory task in the radial maze.

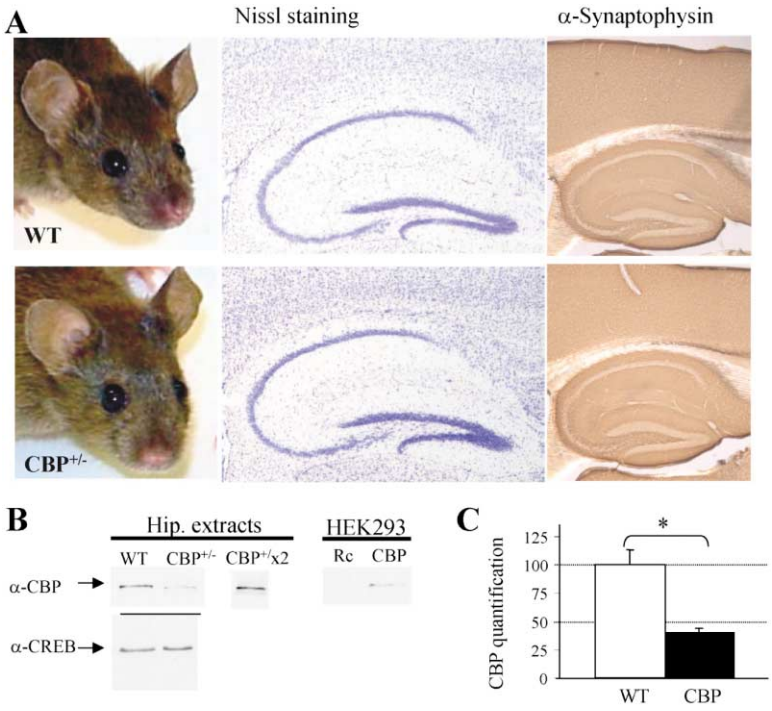

Figure 1. Normal Neuroanatomy and Reduced CBP Level in *cbp*$^{+/-}$ Mice

(A) From left to right: picture of the head of a *cbp*$^{+/-}$ mouse (bottom) and a wild-type littermate (top), Nissl staining of their hippocampus, and immunostaining with α-synaptophysin (sagittal sections).

(B) Western blot of hippocampal protein extracts from *cbp* heterozygous (CBP$^{+/-}$) and control (wt) mice using anti-CBP and anti-CREB antibodies. We observed reduced level of CBP but same level of CREB protein in extracts from mutant mice. CBP$^{+/-}$×2: double amount of extract from a heterozygous mouse. Protein extract of HEK296 cells overexpressing CBP protein was used as positive control: Rc, cells transfected with pRcRSV empty vector (Invitrogen); CBP, cells transfected with pRcRSV.CBP plasmid encoding mouse CBP.

(C) Quantification of Western blot of hippocampal protein extracts from three different CBP$^{+/-}$ (CBP) mice and three control (wt) mice using anti-CBP antibody ($p = 0.009$).

Working memory is a form of transient, short-term memory, and therefore, it is thought to be independent of transcription and new gene expression. Mutant mice and their littermates had a similar learning curve in the radial maze task (Figure 2G and result not shown) and committed a similar number and kind of errors during the task ($p = 0.8$).

cbp$^{+/-}$ Mice Have Reduced Long-Term Memory for Fear and Object Recognition, but Normal Learning in Spatial Navigation

Does the reduced expression of CBP in the hippocampus of *cbp*$^{+/-}$ mice correlate with deficits in forms of long-term memory that involve the activation of CREB? To address this question, we tested these mice in several memory tasks. First, we assessed *cbp*$^{+/-}$ mice in a fear conditioning task that measures the capability of the mouse to form an association between an aversive stimulus and neutral environmental cues. We examined the same mice in two forms of fear conditioning: contextual and cued. During contextual fear conditioning, the animals learn to associate a specific environmental context (conditioned stimulus or CS) with an electric foot shock (unconditioned stimulus or US) that they received there. This memory depends on both hippocampal and amygdalar function and is evaluated by the percentage of time that the animal freezes when re-exposed to the same context. In cued fear conditioning, the animal learns to associate a simple conditioned stimulus (a tone) with a foot shock. This memory depends on the amygdala and not the hippocampus. In agreement with previous findings in mice expressing a truncated CBP protein (Oike et al., 1999a), we found that *cbp*$^{+/-}$ mutants froze less than control mice in both contextual and cued fear conditioning (Figure 3A).

We also assessed *cbp*$^{+/-}$ mice in novel object recognition, a nonaversive memory task that relies on the natural exploratory behavior of mice. In this task, mice were exposed to two identical objects for 15 min during the training session. We tested their memory for these objects at a later time by presenting the mice with two objects, one of them previously used during training and the other a novel item. Wild-type mice remember the familiar object and consequently spend more time exploring the novel object. We then tested *cbp*$^{+/-}$ mutants and control littermates for memory retention and found that *cbp*$^{+/-}$ mutants remembered the familiar object after 3 hr (Figure 3B, top) but not after 24 hr (Figure 3B, bottom), indicating that they have normal short-term memory but impaired long-term memory.

Finally, we examined the performance of *cbp*$^{+/-}$ mice in spatial navigation using the Morris water maze (MWM). We found no significant differences in the visible platform task (Figure 3C), although mutant mice showed a trend to swim slower (Figure 3E). When we assessed spatial learning using the hidden platform version of the water maze, we found no difference in latency and path length between mutant and wild-type littermates, although the mutants showed a tendency for slower swimming during the last days of training (Figures 3C and 3E). This last finding is in agreement with the locomotive deficit observed in the rotarod task.

To examine spatial learning more rigorously, we performed two probe trials, on days 5 and 10. Again, we did not find any statistically significant differences in performance between mutants and wild-type controls (Figure 3G). We then assessed learning flexibility by transferring the platform to a new position and measuring the capability of the mice to learn the new position (Figures 3D and 3F). We found that *cbp*$^{+/-}$ mice are as flexible as control littermates in learning the new platform position after few trials (Figure 3G, bottom). The

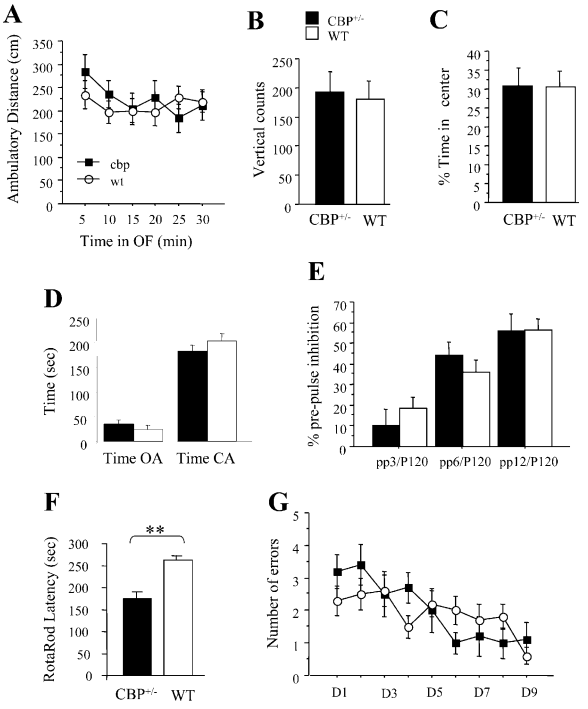

Figure 2. Open Field Behavior, Anxiety, Sensorimotor Gating, and Motor Coordination in *cbp*$^{+/-}$ Mice

(A–C) *cbp*$^{+/-}$ mice behave as control littermates in an open field (wild-type, n = 13; *cbp*$^{+/-}$, n = 14). Ambulatory distance during a 30 min period (A, p = 0.73), vertical counts (B, p = 0.82), and percentage of time spent in the center of the arena (C, p = 0.87) were similar for both genotypes, as well as stereotypic time, resting time, vertical time, and other parameters not shown.

(D) *cbp*$^{+/-}$ mice also showed normal anxiety as measured in the elevated plus maze (wt, n = 14; *cbp*$^{+/-}$, n = 12; p = 0.48).

(E) No difference was observed between genotypes for prepulse inhibition (wt, n = 14; *cbp*$^{+/-}$, n = 12; p = 0.97).

(F) Poor rotarod performance of *cbp*$^{+/-}$ mice (wt, n = 22; *cbp*$^{+/-}$, n = 19; p $<$ 0.0001).

(G) *cbp*$^{+/-}$ mice and control littermates committed a similar number and kind of errors in a working memory task in the radial maze (wt, n = 10; *cbp*$^{+/-}$, n = 10; p = 0.8) (see Experimental Procedures for details).

absence of a memory phenotype in the Morris water maze in spite of the LTM deficits in contextual conditioning and object recognition tasks may be the consequence of the different requirements and structures underlying this form of learning; thus, it is possible that repeated training can overcome the memory deficits observed in tasks dependent on a one-time experience, such as object recognition or fear conditioning.

Thus, our behavioral analysis of *cbp*$^{+/-}$ mutants confirmed the cognitive deficits associated to this condition and illustrated the utility of these mice in modeling RTS symptoms. Our results in fear conditioning and object recognition tasks are similar to those reported for the truncated CBP model, which suggests that a haploinsufficiency mechanism by itself is sufficient to lead to such cognitive deficits.

cbp$^{+/-}$ Mutants Show Normal E-LTP but Deficient L-LTP

Long-term potentiation (LTP) in the Schaffer collateral pathway is an important form of synaptic plasticity that is thought to underlie the storage of spatial memories in the hippocampus (Martin et al., 2000). In LTP, as in memory storage, there is an early, short-term stage (E-LTP), which lasts minutes, and a later, long-term stage (L-LTP), which lasts longer and requires the synthesis of new mRNA and protein (Martin et al., 2000). While it is thought that E-LTP is a local covalent modification in the stimulated synapses, L-LTP requires the participation of the cell nucleus, activation of specific pattern of gene expression, and perhaps chromatin remodeling, since this has now been described for long-term facilitation in *Aplysia* (Guan et al., 2002).

Do the memory deficits observed in *cbp*$^{+/-}$ mice correlate with defects in synaptic plasticity? To address this question, we explored the electrophysiological phenotype of these mice in the Schaffer collateral pathway by recording extracellular field potentials. We found no significant difference in stimulus-response curves and in paired-pulse facilitation (PPF) between *cbp*$^{+/-}$ mutants and wild-type mice (Figures 4A and 4B), indicating that basal transmission is not affected by the mutation.

Although the reduction of CBP appears not to affect basal synaptic transmission, it might affect long-lasting forms of synaptic plasticity that depend on transcriptional activation. To test this idea, we first investigated LTP induction by a standard 100 Hz tetanus train of 1 s duration. A single 100 Hz train produced a nonsaturating, transcription-independent form of LTP lasting about 90 min (E-LTP) in wild-type mice and had similar effects, both in amplitude and duration, in *cbp*$^{+/-}$ mutants (Figure 4C; 20–30 min: wt, 163% ± 6%; *cbp*$^{+/-}$, 164% ± 8%, p = 0.8). Conversely, when we used repeated stimulation consisting of four 100 Hz trains spaced 5 min apart, which is known to induce, in wild-type mice, a form of LTP lasting several hours (L-LTP) and requiring protein and RNA synthesis, *cbp*$^{+/-}$ mice showed a severe deficit in the late phase of L-LTP (Figure 4D; 20–30 min: wt, 205% ± 12%; *cbp*$^{+/-}$, 194% ± 6%, p = 0.15; 120–150 min: 183% ± 5.2% versus 134% ± 7%, p = 0.0006). To test whether this deficit can be overcome by further stimulation, we used a protocol consistent in the repetition of four 100 Hz trains stimulation spaced 30 min apart. This protocol did not further increase LTP in wild-type mice but significantly enhanced the LTP observed in mutant mice (Figure 4E; 150–180 min: *cbp*$^{+/-}{}_{4\text{trains}}$, 128% ± 6%; *cbp*$^{+/-}{}_{2\times4\text{trains}}$, 159% ± 4%, p = 0.002), suggesting that these mice can develop some forms of L-LTP after repeated stimulation.

We next examined long-term depression (LTD) in the Schaffer collateral pathway, a different form of synaptic plasticity. We found that stimulation with one 1 Hz train of 15 min duration evoked LTD with similar amplitude in *cbp*$^{+/-}$ mice and wild-type littermates (Figure 4F). Therefore, the reduced level of CBP produces a specific deficit in the late phase of long-lasting forms of LTP. Our results in the physiology of hippocampal slices correlated with those on behavior: normal generation of E-LTP and short-term memories and impaired formation of L-LTP and some forms of long-term memory.

The Deficit in L-LTP Can Be Ameliorated by Enhancing CREB-Dependent Gene Expression

Are these deficits due to an inefficient induction of gene expression by neuronal activity? To address this ques-

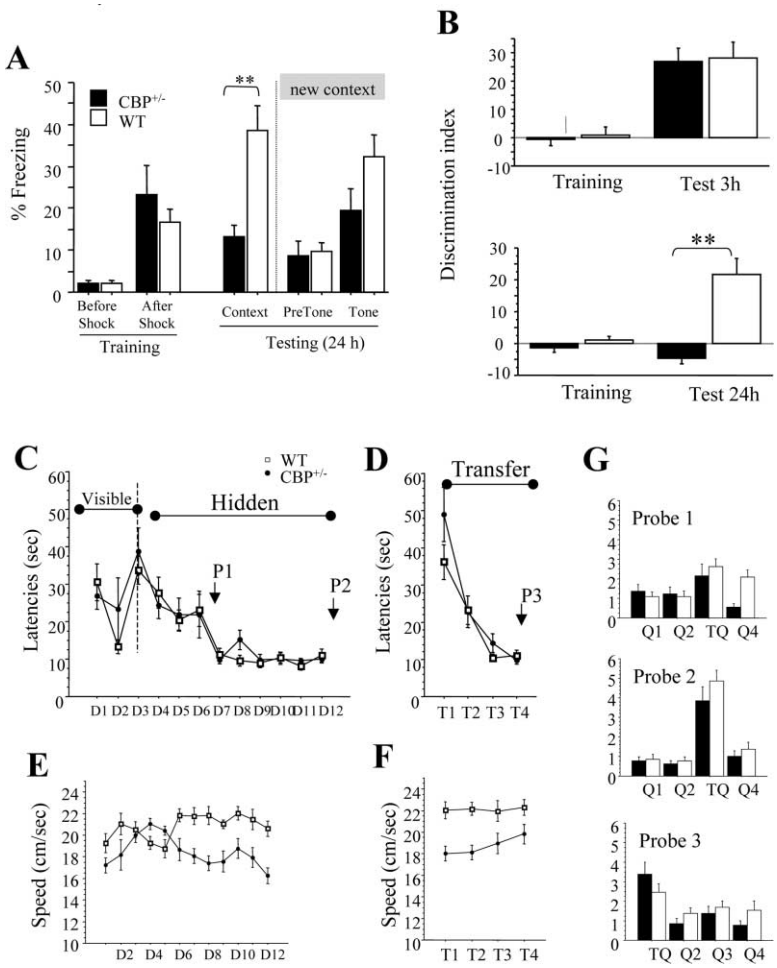

Figure 3. *cbp*$^{+/-}$ Mice Show Reduced Object Recognition and Fear Memories and Normal Spatial Memory in the MWM

(A) Reduced freezing in contextual and cued conditioning 24 hr after training (n = 13 for both genotypes). Both genotypes showed similar immediate freezing after the shock (p = 0.42), but wild-type mice froze more than mutants when re-exposed to the same context (p = 0.0006). In the case of cued conditioning, we observed a clear trend to reduced freezing in *cbp*$^{+/-}$ mice (p = 0.091).

(B) Normal short-term memory for object recognition 3 hr after training (top: wt, n = 8; *cbp*$^{+/-}$, n = 8; p = 0.89). *cbp*$^{+/-}$ mice showed impaired long-term memory for object recognition when tested 24 hr after training (bottom: wt, n = 12; *cbp*$^{+/-}$, n = 12; p < 0.0001).

(C–G) A four-trial per day protocol was used in this experiment. No significant differences between genotypes were observed during training in both the visible platform and the hidden platform tasks (C); moreover, *cbp*$^{+/-}$ mice were also able to learn a new position of the platform during the transfer experiment as well as wild-type mice (D) (n = 13 for both genotypes). However, *cbp*$^{+/-}$ mice showed a significantly slower swimming speed during both tasks (E and F), probably due to a reduced motor coordination, as observed in the rotarod. Spatial memory was assessed in three probe trials (G), and no significant difference was observed. Values represent number of crossings.

tion, we first investigated gene induction by kainate, an analog of L-glutamate that causes depolarization of neurons, severe seizures, and the induction of immediate early genes (IEG). We did not find significant differences in the basal level (Figure 5B, first two columns) or kainate-induced expression (Figure 5A and results not shown) of some well-characterized IEGs, such as brain-derived neurotrophic factor (BDNF), Arc, c-*fos*, and Egr1 (Patterson et al., 1992; Sheng et al., 1990). Since the promoters of some of these IEGs contain CRE sites, this result suggests that the CREB-activation pathway is still largely functional in *cbp*$^{+/-}$ mice, at least when a very strong stimulus is used for its induction.

Next, we investigated whether the L-LTP deficit observed in *cbp*$^{+/-}$ mice is the result of a failure to specifically activate CREB-dependent gene expression. We have recently found that regulated expression of a constitutively active form of CREB, called VP16-CREB, in hippocampal neurons stimulated the transcription of several downstream genes and lowered the threshold for eliciting a persistent late phase of LTP (Barco et al., 2002). Since the VP16 domain can directly engage the transcription machinery, this activation is likely independent of CBP recruitment to a promoter. We crossed VP16-CREB and *cbp*$^{+/-}$ mice and found that the enhanced expression of CREB downstream genes observed in VP16-CREB mice, such as BDNF, dynorphin, or c-*fos* (Barco et al., 2002), also takes place in the VP16-CREB/*cbp*$^{+/-}$ double mutants (Figure 5B). We then analyzed the L-LTP phenotype in hipppocampal slices from double mutants and found that the deficit observed in *cbp*$^{+/-}$ mice was in part ameliorated by VP16-CREB expression (Figures 5C and 5D). In agreement with this result, Bourtchouladze et al. recently reported that the deficit in object recognition observed in truncated-CBP mutant mice was ameliorated by inhibitors of phosphodiesterase 4 (PDE4), which also enhance CREB-dependent gene expression (Barad et al., 1998; Bourtchouladze et al., 2003). To address whether these drugs had a similar effect in the LTP deficit of *cbp*$^{+/-}$ mice, we investigated the effects of preincubation of hippocampal slices from mutant mice with rolipram, a PDE4 inhibitor known to facilitate the establishment of LTP in wild-type mice (Barad et al., 1998). We found, similar to what was observed in the case of VP16-CREB/*cbp*$^{+/-}$ double mutants (Figure 5D), that the deficit in the late phase of LTP was ameliorated but not completely rescued by rolipram (Figure 5E; 150–180 min: *cbp*$^{+/-}$+veh, 126% ± 8%; *cbp*$^{+/-}$+rolipram, 160% ± 9%, p = 0.006).

These results suggest that the L-LTP deficit found in *cbp*$^{+/-}$ mutants, in part, represents an inefficient activation of CREB-dependent genes. However, the fact that the rescue is not complete also implies the contribution of other factors. Although we can not eliminate the possibility that a developmental defect prevents the full expression of L-LTP, an attractive alternative explana-

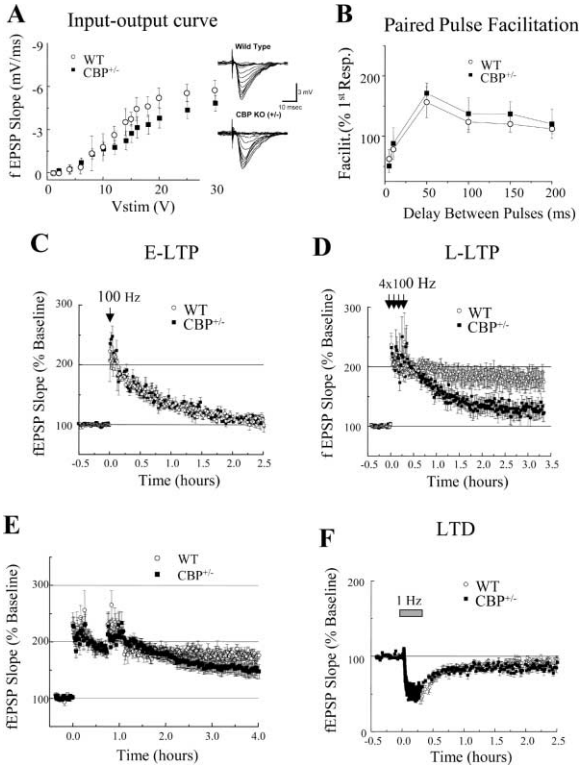

Figure 4. Basal Synaptic Transmission and E-LTP Are Normal in *cbp*$^{+/-}$ Mice, but L-LTP Is Impaired

(A) Input-output curve of fEPSP slope (mV/ms) versus stimulus (V) at the Schaffer collateral pathway of hippocampal slices from heterozygous and control littermates (n = 12 for both genotypes, p = 0.4). Insets show fEPSP responses using increasing stimulation.

(B) Comparison of PPF in mutant and wild-type mice. Data are presented as the mean ± SEM of the facilitation of the second response relative to the first response (n = 10 for both genotypes, p = 0.7).

(C) A single 100 Hz train (1 s) evoked E-LTP in wild-type and mutant animals (n = 6 for both genotypes, p = 0.8).

(D) Four 100 Hz trains stimulation leads to L-LTP in control but not in *cbp* heterozygous mice (n = 8 for both genotypes, p = 0.0006).

(E) Two blocks of 4 × 100 Hz trains stimulation induced a long-lasting form of LTP in both control and mutant mice (n = 5 for both genotypes).

(F) A single 1 Hz train (15 min) evoked LTD in wild-type and mutant animals (n = 6 for both genotypes, p = 0.11).

tion comes from the consideration that CBP has a dual role in transcriptional regulation: CBP directly recruits the Pol II complex to the promoter and it also remodels chromatin by histone acetylation. Thus, VP16-CREB may be bypassing CBP function as scaffold for the transcriptional activation of CRE-dependent gene expression but not its epigenetic role on histone acetylation. Indeed, we did not observe any significant difference in the induction of a CRE-reporter construct by forskolin in transiently transfected primary neuronal cultures from *cbp*$^{+/-}$ control mice (Figure 5F), suggesting that the amount of CBP present in the neurons of *cbp*$^{+/-}$ mice may be sufficient to directly co-activate CRE-driven gene expression. Since transiently transfected DNA is not arranged in regular chromatin arrays and it is either not affected by treatments that alter chromatin remodeling or is affected differently than the chromatin surrounding native genes (Michael et al., 2000; Smith et al., 1997), this result does not rule out a possible deficit in histone acetylation.

Reduced Acetylation of H2B in *cbp*$^{+/-}$ Mice

Nucleosomes are composed of an octameric core consisting of two molecules each of histones H2A, H2B, H3, and H4 wrapped around DNA. The N-terminal unstructured tails of these proteins are the target of histone deacetylases (HDACs) and histone acetyltransferases (HATs), such as CBP, that work in concert to modify chromatin and regulate transcription. Recent findings indicate that CBP acetylates histones in vivo in a concentration-dependent manner affecting large regions of the genome (McManus and Hendzel, 2003). Can the deficits observed in *cbp*$^{+/-}$ mice arise as a consequence of altered chromatin structure due to the reduced activity of CBP? Are the steady-state acetylation levels for the different histones selectively affected in these mutants?

To address these questions, we stained brain sections of wild-type and *cbp*$^{+/-}$ mice with specific anti-acetyl-histone antibodies and we found that acetylation of histone H2B was reduced in mutant mice (Figure 6A). Focusing on the CA1 region of the hippocampus, we found weak immunoreactivity in the nuclei of all pyramidal neurons in both wild-type and *cbp*$^{+/-}$ mice. Whereas control mice had a large number of scattered cells showing intense AcH2B staining in the cellular layer, mutant mice had fewer cells that stained intensely. We confirmed this result by Western blot analysis of hippocampal extracts and found that *cbp*$^{+/-}$ showed an overall reduction of more than 30% in AcH2B levels (Figures 6B and 6C). On the other hand, we did not observe significant changes in the level of acetylation of H2A, H3, and H4, at least, when antibodies that recognize all forms of these acetyl-histones were used (Figure 6). Further characterization using a panel of antibodies against specific acetyl-lysine residues might reveal more alterations in histone acetylation.

The Enhancement of L-LTP and Reversion of Memory Deficit by Inhibition of Histone Deacetylase Activity Suggests a Role for Chromatin Acetylation in Long-Term Plasticity and Memory Storage

Various HDAC inhibitors, such as suberoylanilide hydroxamic acid (SAHA), are currently being tested for their ability to ameliorate the transcriptional deficits in Huntington's disease and in different forms of cancer (Ferrante et al., 2003; Hockly et al., 2003; Kouraklis and Theocharis, 2002). We therefore asked whether HDAC inhibition might compensate for the transcriptional deficits underlying the L-LTP defect observed in *cbp*$^{+/-}$ mice. We found that pretreatment of hippocampal slices with SAHA did not affect the stimulus-response curve (Figure 7A), paired-pulse facilitation (Figure 7B), or the extent of depolarization of the rapid synaptic response elicited during tetanic stimulation (Supplemental Figure S1B at http://www.neuron.org/cgi/content/full/42/6/947/DC1), suggesting that it does not alter basal synaptic transmission. However, SAHA increased the L-LTP induced by 4 × 100 Hz stimulation in both wild-type

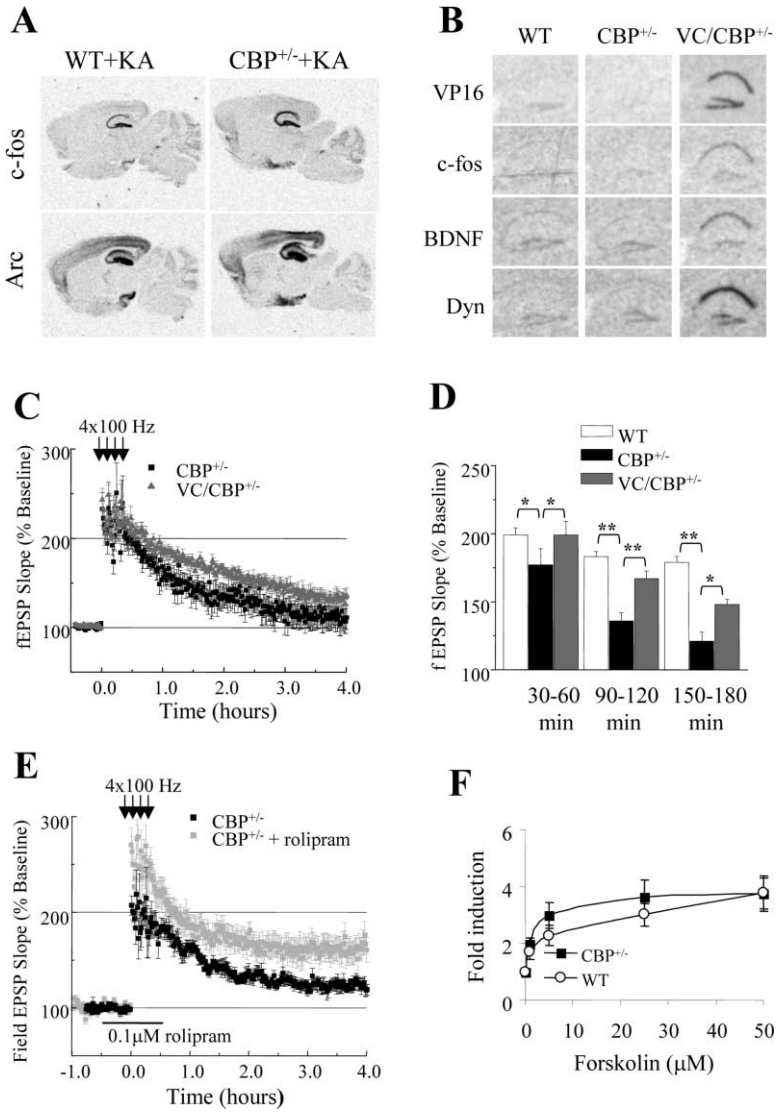

Figure 5. CREB-Dependent Gene Expression in *cbp*$^{+/-}$ Mice

(A) In situ hybridizations using oligo probes specific for the indicated genes on brain sagittal sections from a *cbp*$^{+/-}$ mouse (CBP) and a wild-type littermate (wt) injected with kainic acid 3 hr before sacrificing. Arc promoter does not contain any CRE site, but the promoter of c-*fos*, BDNF, and Erg1 (results not shown) contain one or more CREs.

(B) Oligonucleotide in situs showing enhanced expression of several CRE-dependent genes (namely, c-*fos*, BDNF, and dynorphin) in double mutants with reduced level of CBP and expression of constitutively active CREB (VP16-CREB, indicated as VC in the figure) in the hippocampus. Wild-type (wt) and *cbp*$^{+/-}$ mutants (CBP) showed similar basal level of expression for these genes. Similar results were obtained with 3 independent sets of animals.

(C) Co-expression of VP16-CREB favors the consolidation of LTP induced by four 100 Hz trains in double mutants (wt, n = 5; *cbp*$^{+/-}$, n = 7; VC/*cbp*$^{+/-}$, n = 9).

(D) Columns represent the average amplitude response at the indicated times stimulation (asterisk indicates $p < 0.05$).

(E) Rolipram (0.1 μM) enhances LTP induced by four 100 Hz trains in *cbp*$^{+/-}$ mutants.

(F) Cortical neurons from E19 *cbp*$^{+/-}$ and control embryos were transfected with 1 μg of pCRE.luc reporter plasmid and treated with forskolin, and we did not observe significant differences between the two genotypes. In all transfections, 0.05 μg of pRL-SV40 was added for normalization. TTX 1 μM was added to the culture 16 hr before induction with forskolin. Cells were harvested 3 hr after forskolin treatment. Firefly luciferase expression was normalized to *Renilla* luciferase activity. Similar results were obtained on hippocampal primary cultures from E19 mice (induction fold 3 hr after treatment with 40 μM forskolin: wt = 4.60 ± 1.26, *cbp*$^{+/-}$ = 4.93 ± 0.92).

(Figure 7C; 150–180 min: vehicle, 179% ± 8%; SAHA, 237% ± 8%, $p < 0.005$) and mutant (Figure 7D; 150–180 min: vehicle, 121% ± 7%; SAHA, 210% ± 6%, $p < 0.005$) mice (see also Supplemental Figure S1). Indeed, the level and duration of L-LTP observed in slices of *cbp* heterozygous mice treated with SAHA were similar to that observed in wild-type mice in the absence of the drug (Figure 7E), indicating that this compound can ameliorate the synaptic plasticity deficit observed in mutant mice.

We tested next whether SAHA ameliorates the deficits found in CBP mutants by restoring the basal acetylation steady-state or by inverting the HAT/HDAC balance. To address this question, we analyzed by Western blot the acetylation state of H2B in hippocampal slices treated with SAHA. As previously described (Hockly et al., 2003), we found a strong increase in AcH2B after incubation with the drug (Figure 7E and Supplemental Figure S1D). This increase was similar for both genotypes and closely correlated with our findings in L-LTP.

Finally, we tested the effect of intraventricular infusion of SAHA in fear conditioning, one of the behavioral paradigm affected in *cbp*$^{+/-}$ mutants. We found that injection of the drug 3 hr before training enhanced H2B acetylation (Figures 8A–8D) and enabled *cbp*$^{+/-}$ mice to score in both the cued and contextual task similarly to control mice, reversing the memory deficit observed in contextual fear conditioning (Figure 8E). We also observed a recovery in cued fear conditioning, but in this case the differences were not statistically significant. Our study therefore suggests that it might be possible to use the same HDAC inhibitors that are currently being tested in cancer and Huntington's disease as therapeutic agents for the treatment of RTS.

Discussion

cbp$^{+/-}$ Mice as a Model for Rubinstein-Taybi Syndrome

The Rubinstein-Taybi Syndrome is a complex genetic disorder characterized by stunted growth and mental retardation, skeletal abnormalities including craniofacial malformations, and increased risk of neoplasia. Behavioral studies of patients suffering from Rubinstein-Taybi

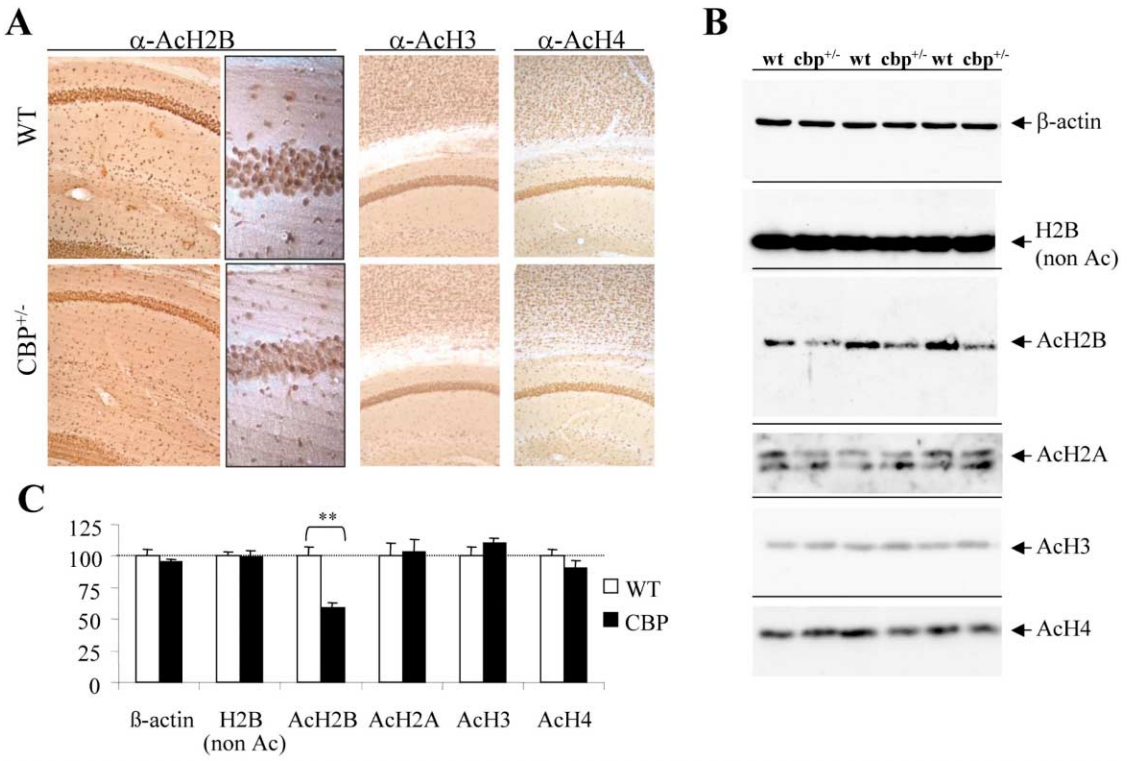

Figure 6. Reduced H2B Acetylation in *cbp*$^{+/-}$ Mice

(A) Immunostaining of sagittal brain sections using antibodies against the acetylated form of histones H2B, H3, and H4 reveals a decreased level of AcH2B in hippocampal neurons (CA1 region shown).

(B) Western blot of hippocampal protein extracts from *cpb*$^{+/-}$ (CBP) and control (wt) mice using α-β-actin (Sigma), α-H2B (nonacetylated, Upstate), α-AcH2B (Upstate), α-AcH2A (Serotec), α-AcH3 (Upstate), and α-AcH4 (Serotec) antibodies.

(C) Quantification of Western blot results. We found no differences in the level of β-actin (6 mice per genotype, $p = 0.4$), total H2B ($n = 6$, $p = 0.97$), AcH2A ($n = 4$, $p = 0.82$), AcH3 ($n = 4$, $p = 0.27$), or AcH4 ($n = 4$, $p = 0.26$), but a significant difference in the level of AcH2B (Upstate Antibody; 6 mice per genotype, $p = 0.001$). We also observed a similar reduction in H2B acetylation using an AcH2B antibody produced by Serotec (wt, 100% ± 8% and *cbp*$^{+/-}$, 71% ± 7%, $p = 0.022$).

syndrome have revealed that their intelligence is low and their attention span short and that they experience difficulty in planning and executing motor acts (Gotts and Liemohn, 1977; Hennekam et al., 1992). Although some of these features cannot be modeled in mice, others, such as the cognitive deficits and reduced motor skills, can be easily assessed. Our results in *cbp*$^{+/-}$ mice demonstrate the suitability of this animal model for gaining new insights in the molecular etiology of the syndrome and for developing new therapeutic approaches. Future studies using region-specific and inducible knockouts and transgenic mice expressing dominant-negative forms of CBP should allow one to investigate the identity of the brain regions involved in the different aspects of the behavioral deficit and the selective contribution to the disease of developmental as opposed to the chronic effects of reduction in CBP.

Molecular Etiology of RTS

Our findings on the haploinsufficiency model of RTS and those by Bourtchouladze and colleagues on the truncated CBP model (Bourtchouladze et al., 2003) indicate that the cognitive deficits observed in *cbp* heterozygous mutants may be a consequence of a reduced level of CBP available to regulate changes in gene expression driven by neuronal activity. However, the specific molecular mechanisms underlying these deficits remain unclear. Based on their finding that PDE4 inhibitors ameliorate these deficits, Bourtchoulatdze and colleagues proposed a role for CREB/CBP interaction in the etiology of behavioral deficits in mutant mice carrying a truncated form of CBP (Bourtchouladze et al., 2003). Our results with rolipram and with VP16-CREB/*cbp*$^{+/-}$ double mutants support a role of CREB-driven gene expression on the etiology of RTS. However, CBP plays a dual role in transcription regulation: it not only recruits the Pol II complex to the promoter, it also remodels chromatin by histone acetylation. Its role on chromatin remodeling may importantly contribute to the phenotype of *cbp*$^{+/-}$ mice. The reduction of CBP may lead to an altered chromatin configuration in one or several loci important for LTP and for memory storage and may interfere with the transcriptional response driven by neuronal stimulation.

The two transcriptional functions of CBP have been dissociated before in the context of mutations identified in RTS patients. Thus, mutations in the HAT domain of CBP completely blocked HAT activity, but only reduced, to about a 50%, its activity as a CREB coactivator (Kalkhoven et al., 2003). Our results in *cbp*$^{+/-}$ mutants sug-

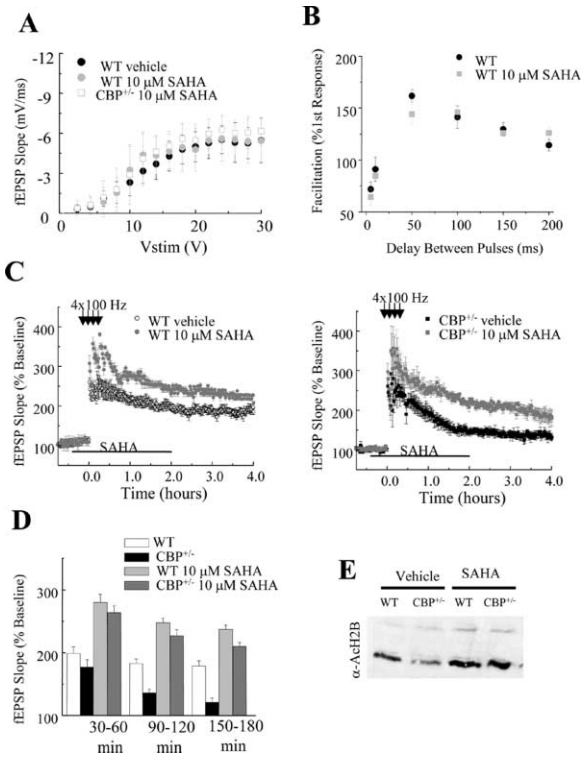

Figure 7. Inhibition of HDAC Enhances L-LTP in Wild-Type Mice

(A) Input-output curve of fEPSP slope (mV/ms) versus stimulus (V) at the Schaffer collateral pathway of hippocampal slices from heterozygous and control littermates treated with 10 μM of SAHA or with vehicle alone (wt vehicle, n = 5; wt SAHA, n = 6; *cbp*$^{+/-}$ vehicle, n = 5; *cbp*$^{+/-}$ SAHA, n = 6).

(B) Comparison of PPF in mutant and wild-type mice in the presence of SAHA. Data are presented as the mean ± SEM of the facilitation of the second response relative to the first response (n = 5 for both genotypes).

(C) SAHA treatment enhances L-LTP induced by four 100 Hz trains in wild-type mice (left; wt vehicle, n = 5; wt SAHA, n = 6) and enables the induction of L-LTP by four 100 Hz trains in *cbp*$^{+/-}$ mutants (right; *cbp*$^{+/-}$ vehicle, n = 5; *cbp*$^{+/-}$ SAHA, n = 6).

(D) Columns represent the average amplitude response at the indicated times stimulation.

(E) Western blot using α-AcH2B antibody of protein extracts from 400 μm acute hippocampal slices of *cbp*$^{+/-}$ and wild-type mice treated or not with 10 μM of SAHA for 30 min. This experiment was repeated three times with similar results.

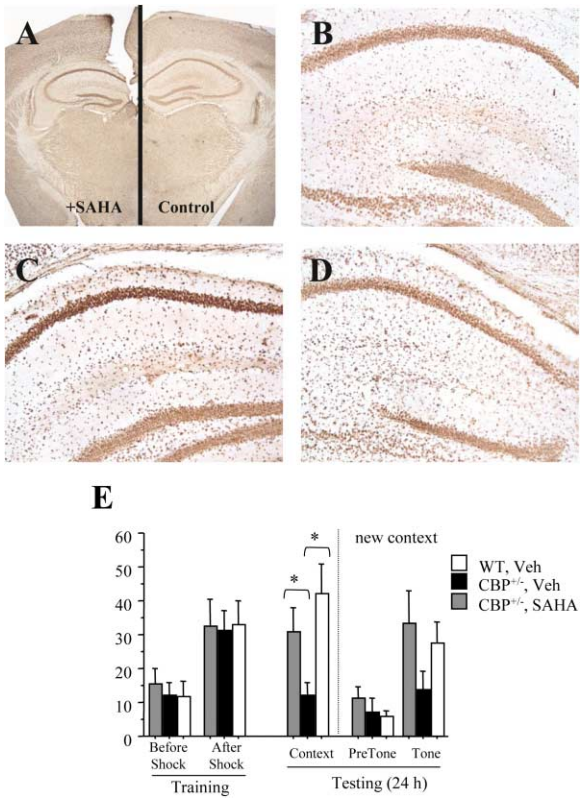

Figure 8. Increased H2B Acetylation and Fear Memory in *cbp*$^{+/-}$ Mice

(A–D) α-AcH2B immunostaining of coronal brain sections 3 hr after intraventricular injection of SAHA (20 μg) revealed a increased level of AcH2B. Strikingly, this increase is especially noticeable in CA1 pyramidal neurons, although it is also clearly observed in cortical neurons (A) (left, *cbp*$^{+/-}$ mouse injected with SAHA; right, *cbp*$^{+/-}$ mouse injected with vehicle). (B)–(D) show the CA1 region of *cbp*$^{+/-}$ mice injected with vehicle (B) or treated with SAHA either 3 hr (C) or 20 hr (D) after injection. 20 hr after injection of SAHA, the acetylation level of H2B was similar to the level observed in untreated animals.

(E) The reduced freezing in contextual conditioning 24 hr after training (CF) observed in *cbp*$^{+/-}$ mice (Figure 3A) was confirmed in mice injected with vehicle (wt+veh: n = 6, CF = 42.0%; *cbp*$^{+/-}$+veh: n = 7, CF = 12.2%; p = 0.008) and reversed by intraventricular injection of 20 μg of SAHA (*cbp*$^{+/-}$+SAHA: n = 9, CF = 31.0%, p = 0.048 when compared with *cbp*$^{+/-}$+veh; p = 0.35 when compared with wt+veh). The trends observed in the case of cued fear conditioning are not statistically significant (wt versus *cbp*$^{+/-}$+veh, p = 0.113; *cbp*$^{+/-}$+SAHA versus *cbp*$^{+/-}$+veh, p = 012).

gest that a reduction of 50% on CBP does not impair the expression of a transiently transfected CRE reporter or the induction of IEGs by kainate and VP16-CREB but strikingly affects the acetylation level of the histone H2B.

A recent study indicates that acetylation of H2B is a feature of only the most active genes (Myers et al., 2003). Indeed, Myers et al. found that acetylation of H2B was widespread and not limited to the promoter, suggesting that this acetylation may have a role in the maintenance of the overall transcriptional competence of the locus (Myers et al., 2003). In vitro experiments have revealed that prior acetylation of nucleosome arrays does not enhance the binding of chromatin remodeling complexes but allows the retention of the complex after the critical transcriptional activator that recruited it has left the promoter, thereby providing a mechanism for epigenetic marking of the chromatin (Hassan et al., 2001). Such markings may well underlie the long-term transcriptional effects in specific loci required for long-term modification of synaptic function. Although in preliminary experiments we have not found differences in the response of any specific endogenous gene in CBP mutants, it is likely that only a subpopulation of genes is affected by the CBP mutation, specifically those genes in which CBP is recruited to the promoter and leaves an epigenetic mark in the form of changes in the acetylation of specific histone residues. These events likely depend on both the primary sequence of the promoter and its previous history of transcriptional activation. The analysis of *cbp*$^{+/-}$ mice using both expression and

acetylation (intergenic) microarrays would allow the identification of these target genes.

Recent studies by McManus and Hendzel on CBP and p300-induced histone acetylation in vivo revealed the unique substrate specificity profiles of these two histone acetyl-transferases (McManus and Hendzel, 2003). Interestingly, they found H2B among the top four acetylated histone species in which the steady state of acetylation was more significantly altered in response to overexpression of both CBP and p300. In the case of $cbp^{+/-}$ mice, we only found a significant deficit in the case of bulk H2B acetylation; however, we cannot rule out the existence of additional differences affecting the acetylation of specific residues in H2A, H2B, H3, and H4. More than 15 lysine residues are targets for acetylation, and we did not investigate the specific effect of CBP reduction in each one of them. It is also likely that the effect in acetylation for some of these residues would be only noticeable in ChIP assays for specific target promoters. Detailed immunohistological analyses of $cbp^{+/-}$ mutants using antibodies against specific acetyl-Lys residues on the different histones and the extension of these analyses to other mouse mutants in HAT and HDAC genes should aid in the analysis of the histone code.

Epigenetics and Human Disease

The affinity between DNA and histones in eukaryotic nucleosomes is modulated by phosphorylation, ubiquitination, methylation, and acetylation of the amino termini of histones. The conformational states of these histone tails determine the transcriptional activity of different chromatin domains and their accessibility to transcription factors and other DNA-associated proteins (Huang et al., 2003). Rubinstein-Taybi syndrome is only one of several neurological diseases that arise as a consequence of disordered chromatin remodeling. Other congenital syndromes that cause mental retardation in humans share a similar type of defect. Thus, Coffin-Lowry syndrome (CLS), X-linked α-thalassemia (ETRX), and Rett syndrome (RT) are conditions that are also caused by mutations in genes encoding enzymes that mediate chromatin remodeling and affect the acetylation state of chromatin indirectly. Coffin-Lowry syndrome results from mutations in the gene encoding RSK2, an enzyme that interacts with CBP and phosphorylates histone H3 favoring its acetylation (Merienne et al., 2001; Trivier et al., 1996). Rett syndrome is caused by mutations of MECP2, a methyl-CpG binding protein that is thought to recruit HDACs to methylated DNA and mediate chromatin deacetylation (Nan et al., 1997). These mutations likely result in deregulation of the expression of a very large number of genes and yet they lead, surprisingly, to a well-defined phenotype. It is therefore likely that specific features of these syndromes are the consequence of dysregulation of perhaps a very few specific target genes. The overlap in the clinical features of these syndromes suggests the possibility that these conditions may share common molecular mediators. A comparison of phenotypic features of different mouse models for these syndromes combined with their molecular characterization using expression and acetylation arrays may reveal some of the common target genes involved in the cognitive disorders and thereby provide valuable information about the etiology of these diseases.

Our experiments with SAHA, a broad HDAC inhibitor, indicate that therapeutical approaches for the treatment of diseases of epigenetic etiology might be possible. It is encouraging that a family of drugs that is currently being tested both in the treatment of cancer (Kouraklis and Theocharis, 2002) and neurodegenerative diseases (Ferrante et al., 2003; Hockly et al., 2003) may enhance L-LTP significantly both in *cbp*-deficient mutants and control littermates. Moreover, HDAC inhibitors reversed the deficit in fear conditioning of $cbp^{+/-}$ mutants. Further studies should reveal if they also improve the performance of wild-type mice. A number of biotech companies are working to improve the specificity and to reduce the side effects of HDAC inhibitors. If these goals are finally accomplished, it would be worthwhile to test the effectiveness of the new drugs in the treatment of Rubinstein-Taybi patients. On the other hand, changes in CBP function have been associated with diverse neurodegenerative conditions, including Huntington's disease (HD) and familial Alzheimer's disease (FAD). While HD has been associated with a reduction in CBP activity (McCampbell et al., 2000; Nucifora et al., 2001), FAD mutations may cause a gain of transcriptional function (Marambaud et al., 2003). Both conditions lead to neurodegeneration, suggesting that caution needs to be exercised in clinical studies involving pharmacological manipulation of CBP activity.

In conclusion, $cbp^{+/-}$ mice show a severe defect in hippocampal synaptic plasticity paralleling their deficits in some forms of long-term memory. Our data and those by Bourtchouladze et al. suggest that some deficits observed in *cbp* mutants can be ameliorated using inhibitors of enzymes that compensate for a reduction in CBP function as CREB co-activator (such as rolipram). But, in addition, our data indicate a second deficit in histone acetylation. As a result, it is also possible to compensate for the reduction in CBP by inhibiting histone deacetylases, the enzymes that counteract CBP role in chromatin remodeling. These findings may open the possibility of dual pharmacological treatment for the neurological deficits observed in RTS patients that reestablish normal CBP function and alleviate some of their symptoms.

Experimental Procedures

Animals

The generation of $cbp^{+/-}$ mice was described before (Tanaka et al., 1997). We observed a progressively reduced transmission of the mutation when the mice were repeatedly backcrossed with C57BL/6J strain (after four backcrossing, many heterozygous males did not transmit and those transmitting exhibited a transmission rate lower than 50%). We therefore decided to carry out our experiments in a genetic background closer to the one used on the original publication with these mice and crossed C57BL/6 mutant males with BALB/c females to generate the F1 hybrids used in our experiments. The wild-type mice used as control groups were, in all cases, littermates of the $cbp^{+/-}$ mice. Mice were maintained and bred under standard conditions, consistent with National Institutes of Health guidelines and approved by the Institutional Animal Care and Use Committees.

Western Blot, Immunohistochemistry, and In Situ Hybridization

Nissl staining, hippocampal protein extracts, and Western blot analysis were carried out as previously described (Mayford et al., 1996).

Anti-CBP antibody was obtained from Santa Cruz Biotech and the different acetyl-histone antibodies were obtained from Upstate and Serotec. For immunohistochemistry, mice were anesthetized, perfused with 4% paraformaldehyde, and postfixed overnight, and 50 μm sections were obtained using a vibratome. Staining with DAB was carried out according to the ABC kit (Vector). In situ hybridization was performed as described using [^{33}P]ATP-labeled oligonucleotides specific for the different genes analyzed (Wisden and Morris, 1994).

Electrophysiology

Hippocampi were collected following cervical dislocation of 3- to 4-month-old mice of either sex. Transverse hippocampal slices (400 μm) were incubated in an interface chamber at 27°C–28°C, subfused with oxygenated artificial cerebrospinal fluid (ACSF, containing 119 mM NaCl, 2.3 mM KCl, 1.3 mM $MgSO_4$, 2.5 mM $CaCl_2$, 26.2 mM $NaHCO_3$, 1 mM NaH_2PO_4, and 11 mM glucose), and allowed to equilibrate for at least 90 min. When indicated, ACSF was supplemented with SAHA (BioVision, Inc.) or rolipram (Sigma-RBI). For recording of fEPSP in the CA1 region of the hippocampus, both the stimulating and recording electrodes were placed in the stratum radiatum of CA1 area. The stimulation intensity (0.05 ms duration) was adjusted to give fEPSP slopes approximately 40% of the maximum, and baseline responses were elicited once per minute at this intensity. In all electrophysiological experiments, "n" indicates the number of slices, and two-way ANOVA and Student's t test were used for data analysis. In the text, the electrophysiological data were presented as mean ± SD, whereas in the figures the values were presented as mean ± SEM. Experimenter was blind to mice genotype.

Behavior

For all behavioral tasks, we used adult male mutant and control littermates. Statistical analyses used ANOVAs and means ± SEM are presented in the figures. The experimenters were blind to the genotype in all studies.

Open Field

Mice were placed in 40 × 40 cm^2 open-field chambers and monitored throughout the test session (30 min) by a video-tracking system. (PolyTrack, San Diego Instruments, San Diego, CA), which monitors up to four animals simultaneously and records the position of each animal every 0.5 s.

Anxiety Test

Mice were placed in the center of the elevated plus maze, and their behavior was recorded for 5 min with a camera located above the maze. Times spent and entries in the different compartments (closed and open arms) were assessed.

Prepulse Inhibition

Animals were placed in startle chambers where a high-frequency speaker produced the acoustic stimuli. A piezoelectric accelerometer mounted under each chamber detected and transduced animal movements. Five different trial types were presented during a test session: a 40 ms broadband 120 dB burst (pulse alone trial); three different prepulse + pulse trials in which 20 ms long 3, 6, or 12 dB stimuli above the 65 dB background preceded the 120 dB pulse by 100 ms; and a no stimulus trial, in which only the background noise was presented. PPI was calculated as the averaged startle magnitude on pulse-alone trials, minus the averaged startle magnitude on prepulse/pulse trials, all divided by the averaged pulse-alone values. Graph represents percentage PPI values.

Rotarod

Mice were first trained on an Ugo Basile accelerating rotarod at a constant speed (~20 rpm). Mice received three trials per day for 2 days. A steady level of performance was attained in both genotypes. On the testing day, the rotarod was set to increase from 4 to 40 rpm over 300 s, and the interval for mice to fall off was measured.

Working Memory in the Radial Maze

Food-deprived males (90% of free-feeding weight) were habituated for a week to retrieve food pellets in cups placed at the end of each arm of an elevated 8-arm radial maze. During the training phase, mice were allowed to visit 4 arms (randomly chosen every day). In the subsequent testing phase, the eight arms of the maze were opened. Working memory errors (runs into an already visited arm) and latency to perform the task were recorded during the testing phase.

Fear Conditioning

On the training day, the mice were placed in the conditioning chamber for 2 min before the onset of CS, a tone at 2800 Hz, 85 dB, which lasted for 30 s. The last 2 s of the CS were paired with US, 0.7 mA of continuous foot shock. After an additional 30 s in the chamber, mice were returned to their home cage. Conditioning was assessed 24 hr later by scoring freezing behavior using a video tracking system. Testing occurred first in the context in which mice were trained (contextual fear conditioning) and 3 hr later in a novel environment where, after a 1 min habituation period, the tone that was presented during training was given during 120 s (cued fear conditioning). To test the effect of SAHA, mice were anesthetized (0.5 ml of 2.5% avertin per mouse, i.p.), and stereotaxic procedures were used to implant stainless steel guide cannulae into both lateral ventricles. The stereotaxic coordinates were 0.2 mm posterior to the Bregma, 1.4 mm lateral to the sagittal line, and 1.9 mm ventral from the surface of the skull. After a week recovery, the stylus was removed and a stainless steel internal cannula, connected to a Hamilton microsyringe via tubing, was inserted. The tip of the injection cannula protruded 0.5 mm beyond that of the guide. Freely moving mice received intracerebroventricular (i.c.v.) injection of 2 μl (1 μl per ventricle) of 2-hydroxypropyl-β-cyclodextrin (50% v/v) alone (vehicle) or containing 20 μg of SAHA (BioVision Inc.) at the rate of 1 μl/90 s. Three hours later, we trained the mice for fear conditioning as described above. One of the mice injected with SAHA died 24 hr after testing and was not considered in our analysis.

Object Recognition

This task was performed as previously described (Bourtchouladze et al., 2003): mice were tested at 3 and 24 hr. The discrimination index was determined as the difference in exploration time expressed as a ratio of the total time spent exploring the two objects.

Water Maze

The task was performed as previously described (Malleret et al., 1999). Four trials, 120 s maximum and 15 min ITI (intertrial interval) were given daily. Probe trials (60 s), during which the platform was removed, were performed to assess retention of the previously acquired information.

Acknowledgments

The authors thank Amit Etkin, Christoph Kellendonk, Matt Nolan, Sally Till, and other members of the Kandel lab for critical reading of the manuscript and for helpful comments. We thank Zhonghui Guan and Benny Chih for their help and Brian Skorney, Bing Liu, and Perminder Khosa for excellent technical assistance. A.B. is supported by a grant from the Hereditary Disease Foundation. E.R.K is supported by Howard Hughes Medical Institute, by the G. Harold and Leila Y. Mathers Foundation, and by Columbia University Alzheimer's Research Center grant P50 AG08702. The authors of this paper have declared a conflict of interest. For details, go to http://www.neuron.org/cgi/content/full/42/6/947/DC1.

Received: December 1, 2003
Revised: March 16, 2004
Accepted: April 8, 2004
Published: June 23, 2004

References

Bannister, A.J., Oehler, T., Wilhelm, D., Angel, P., and Kouzarides, T. (1995). Stimulation of c-Jun activity by CBP: c-Jun residues Ser63/73 are required for CBP induced stimulation in vivo and CBP binding in vitro. Oncogene *11*, 2509–2514.

Barad, M., Bourtchouladze, R., Winder, D.G., Golan, H., and Kandel, E. (1998). Rolipram, a type IV-specific phosphodiesterase inhibitor, facilitates the establishment of long-lasting long-term potentiation and improves memory. Proc. Natl. Acad. Sci. USA *95*, 15020–15025.

Barco, A., Alarcon, J.M., and Kandel, E.R. (2002). Expression of constitutively active CREB protein facilitates the late phase of long-term potentiation by enhancing synaptic capture. Cell *108*, 689–703.

Bourtchouladze, R., Lidge, R., Catapano, R., Stanley, J., Gossweiler,

S., Romashko, D., Scott, R., and Tully, T. (2003). A mouse model of Rubinstein-Taybi syndrome: defective long-term memory is ameliorated by inhibitors of phosphodiesterase 4. Proc. Natl. Acad. Sci. USA *100*, 10518–10522.

Chan, H.M., and La Thangue, N.B. (2001). p300/CBP proteins: HATs for transcriptional bridges and scaffolds. J. Cell Sci. *114*, 2363–2373.

Chrivia, J.C., Kwok, R.P., Lamb, N., Hagiwara, M., Montminy, M.R., and Goodman, R.H. (1993). Phosphorylated CREB binds specifically to the nuclear protein CBP. Nature *365*, 855–859.

Coupry, I., Roudaut, C., Stef, M., Delrue, M.A., Marche, M., Burgelin, I., Taine, L., Cruaud, C., Lacombe, D., and Arveiler, B. (2002). Molecular analysis of the CBP gene in 60 patients with Rubinstein-Taybi syndrome. J. Med. Genet. *39*, 415–421.

Ferrante, R.J., Kubilus, J.K., Lee, J., Ryu, H., Beesen, A., Zucker, B., Smith, K., Kowall, N.W., Ratan, R.R., Luthi-Carter, R., and Hersch, S.M. (2003). Histone deacetylase inhibition by sodium butyrate chemotherapy ameliorates the neurodegenerative phenotype in Huntington's disease mice. J. Neurosci. *23*, 9418–9427.

Gerritsen, M.E., Williams, A.J., Neish, A.S., Moore, S., Shi, Y., and Collins, T. (1997). CREB-binding protein/p300 are transcriptional coactivators of p65. Proc. Natl. Acad. Sci. USA *94*, 2927–2932.

Gotts, E.E., and Liemohn, W.P. (1977). Behavioral characteristics of three children with the broad thumb-hallux (Rubinstein-Taybi) syndrome. Biol. Psychiatry *12*, 413–423.

Guan, Z., Giustetto, M., Lomvardas, S., Kim, J.H., Miniaci, M.C., Schwartz, J.H., Thanos, D., and Kandel, E.R. (2002). Integration of long-term-memory-related synaptic plasticity involves bidirectional regulation of gene expression and chromatin structure. Cell *111*, 483–493.

Hassan, A.H., Neely, K.E., and Workman, J.L. (2001). Histone acetyltransferase complexes stabilize swi/snf binding to promoter nucleosomes. Cell *104*, 817–827.

Hennekam, R.C., Baselier, A.C., Beyaert, E., Bos, A., Blok, J.B., Jansma, H.B., Thorbecke-Nilsen, V.V., and Veerman, H. (1992). Psychological and speech studies in Rubinstein-Taybi syndrome. Am. J. Ment. Retard. *96*, 645–660.

Herdegen, T., and Leah, J.D. (1998). Inducible and constitutive transcription factors in the mammalian nervous system: control of gene expression by Jun, Fos and Krox, and CREB/ATF proteins. Brain Res. Brain Res. Rev. *28*, 370–390.

Hockly, E., Richon, V.M., Woodman, B., Smith, D.L., Zhou, X., Rosa, E., Sathasivam, K., Ghazi-Noori, S., Mahal, A., Lowden, P.A., et al. (2003). Suberoylanilide hydroxamic acid, a histone deacetylase inhibitor, ameliorates motor deficits in a mouse model of Huntington's disease. Proc. Natl. Acad. Sci. USA *100*, 2041–2046.

Hu, S.C., Chrivia, J., and Ghosh, A. (1999). Regulation of CBP-mediated transcription by neuronal calcium signaling. Neuron *22*, 799–808.

Huang, C., Sloan, E.A., and Boerkoel, C.F. (2003). Chromatin remodeling and human disease. Curr. Opin. Genet. Dev. *13*, 246–252.

Impey, S., Fong, A.L., Wang, Y., Cardinaux, J.R., Fass, D.M., Obrietan, K., Wayman, G.A., Storm, D.R., Soderling, T.R., and Goodman, R.H. (2002). Phosphorylation of CBP mediates transcriptional activation by neural activity and CaM kinase IV. Neuron *34*, 235–244.

Janknecht, R., and Nordheim, A. (1996). MAP kinase-dependent transcriptional coactivation by Elk-1 and its cofactor CBP. Biochem. Biophys. Res. Commun. *228*, 831–837.

Kalkhoven, E., Roelfsema, J.H., Teunissen, H., den Boer, A., Ariyurek, Y., Zantema, A., Breuning, M.H., Hennekam, R.C., and Peters, D.J. (2003). Loss of CBP acetyltransferase activity by PHD finger mutations in Rubinstein-Taybi syndrome. Hum. Mol. Genet. *12*, 441–450.

Kandel, E.R. (2001). The molecular biology of memory storage: a dialogue between genes and synapses. Science *294*, 1030–1038.

Kouraklis, G., and Theocharis, S. (2002). Histone deacetylase inhibitors and anticancer therapy. Curr. Med. Chem. Anti-Canc. Agents *2*, 477–484.

Lonze, B.E., and Ginty, D.D. (2002). Function and regulation of CREB family transcription factors in the nervous system. Neuron *35*, 605–623.

Lu, Q., Hutchins, A.E., Doyle, C.M., Lundblad, J.R., and Kwok, R.P. (2003). Acetylation of cAMP-responsive element-binding protein (CREB) by CREB-binding protein enhances CREB-dependent transcription. J. Biol. Chem. *278*, 15727–15734.

Malleret, G., Hen, R., Guillou, J.L., Segu, L., and Buhot, M.C. (1999). 5–HT1B receptor knock-out mice exhibit increased exploratory activity and enhanced spatial memory performance in the Morris water maze. J. Neurosci. *19*, 6157–6168.

Marambaud, P., Wen, P.H., Dutt, A., Shioi, J., Takashima, A., Siman, R., and Robakis, N.K. (2003). A CBP binding transcriptional repressor produced by the PS1/epsilon-cleavage of N-cadherin is inhibited by PS1 FAD mutations. Cell *114*, 635–645.

Martin, S.J., Grimwood, P.D., and Morris, R.G. (2000). Synaptic plasticity and memory: an evaluation of the hypothesis. Annu. Rev. Neurosci. *23*, 649–711.

Mayford, M., Bach, M.E., Huang, Y.Y., Wang, L., Hawkins, R.D., and Kandel, E.R. (1996). Control of memory formation through regulated expression of a CaMKII transgene. Science *274*, 1678–1683.

McCampbell, A., Taylor, J.P., Taye, A.A., Robitschek, J., Li, M., Walcott, J., Merry, D., Chai, Y., Paulson, H., Sobue, G., and Fischbeck, K.H. (2000). CREB-binding protein sequestration by expanded polyglutamine. Hum. Mol. Genet. *9*, 2197–2202.

McManus, K.J., and Hendzel, M.J. (2003). Quantitative analysis of CBP- and P300-induced histone acetylations in vivo using native chromatin. Mol. Cell. Biol. *23*, 7611–7627.

Merienne, K., Pannetier, S., Harel-Bellan, A., and Sassone-Corsi, P. (2001). Mitogen-regulated RSK2-CBP interaction controls their kinase and acetylase activities. Mol. Cell. Biol. *21*, 7089–7096.

Michael, L.F., Asahara, H., Shulman, A.I., Kraus, W.L., and Montminy, M. (2000). The phosphorylation status of a cyclic AMP-responsive activator is modulated via a chromatin-dependent mechanism. Mol. Cell. Biol. *20*, 1596–1603.

Myers, F.A., Chong, W., Evans, D.R., Thorne, A.W., and Crane-Robinson, C. (2003). Acetylation of histone H2B mirrors that of H4 and H3 at the chicken beta-globin locus but not at housekeeping genes. J. Biol. Chem. *278*, 36315–36322.

Nan, X., Campoy, F.J., and Bird, A. (1997). MeCP2 is a transcriptional repressor with abundant binding sites in genomic chromatin. Cell *88*, 471–481.

Nucifora, F.C., Jr., Sasaki, M., Peters, M.F., Huang, H., Cooper, J.K., Yamada, M., Takahashi, H., Tsuji, S., Troncoso, J., Dawson, V.L., et al. (2001). Interference by huntingtin and atrophin-1 with cbp-mediated transcription leading to cellular toxicity. Science *291*, 2423–2428.

Oike, Y., Hata, A., Mamiya, T., Kaname, T., Noda, Y., Suzuki, M., Yasue, H., Nabeshima, T., Araki, K., and Yamamura, K. (1999a). Truncated CBP protein leads to classical Rubinstein-Taybi syndrome phenotypes in mice: implications for a dominant-negative mechanism. Hum. Mol. Genet. *8*, 387–396.

Oike, Y., Takakura, N., Hata, A., Kaname, T., Akizuki, M., Yamaguchi, Y., Yasue, H., Araki, K., Yamamura, K., and Suda, T. (1999b). Mice homozygous for a truncated form of CREB-binding protein exhibit defects in hematopoiesis and vasculo-angiogenesis. Blood *93*, 2771–2779.

Parker, D., Ferreri, K., Nakajima, T., LaMorte, V.J., Evans, R., Koerber, S.C., Hoeger, C., and Montminy, M.R. (1996). Phosphorylation of CREB at Ser-133 induces complex formation with CREB-binding protein via a direct mechanism. Mol. Cell. Biol. *16*, 694–703.

Patterson, S.L., Grover, L.M., Schwartzkroin, P.A., and Bothwell, M. (1992). Neurotrophin expression in rat hippocampal slices: a stimulus paradigm inducing LTP in CA1 evokes increases in BDNF and NT-3 mRNAs. Neuron *9*, 1081–1088.

Perkins, N.D., Felzien, L.K., Betts, J.C., Leung, K., Beach, D.H., and Nabel, G.J. (1997). Regulation of NF-kappaB by cyclin-dependent kinases associated with the p300 coactivator. Science *275*, 523–527.

Petrij, F., Giles, R.H., Dauwerse, H.G., Saris, J.J., Hennekam, R.C., Masuno, M., Tommerup, N., van Ommen, G.J., Goodman, R.H., Pe-

ters, D.J., et al. (1995). Rubinstein-Taybi syndrome caused by mutations in the transcriptional co-activator CBP. Nature *376*, 348–351.

Petrij, F., Dauwerse, H.G., Blough, R.I., Giles, R.H., van der Smagt, J.J., Wallerstein, R., Maaswinkel-Mooy, P.D., van Karnebeek, C.D., van Ommen, G.J., van Haeringen, A., et al. (2000). Diagnostic analysis of the Rubinstein-Taybi syndrome: five cosmids should be used for microdeletion detection and low number of protein truncating mutations. J. Med. Genet. *37*, 168–176.

Sheng, M., McFadden, G., and Greenberg, M.E. (1990). Membrane depolarization and calcium induce c-fos transcription via phosphorylation of transcription factor CREB. Neuron *4*, 571–582.

Smith, C.L., Htun, H., Wolford, R.G., and Hager, G.L. (1997). Differential activity of progesterone and glucocorticoid receptors on mouse mammary tumor virus templates differing in chromatin structure. J. Biol. Chem. *272*, 14227–14235.

Tanaka, Y., Naruse, I., Maekawa, T., Masuya, H., Shiroishi, T., and Ishii, S. (1997). Abnormal skeletal patterning in embryos lacking a single Cbp allele: a partial similarity with Rubinstein-Taybi syndrome. Proc. Natl. Acad. Sci. USA *94*, 10215–10220.

Tanaka, Y., Naruse, I., Hongo, T., Xu, M., Nakahata, T., Maekawa, T., and Ishii, S. (2000). Extensive brain hemorrhage and embryonic lethality in a mouse null mutant of CREB-binding protein. Mech. Dev. *95*, 133–145.

Trivier, E., De Cesare, D., Jacquot, S., Pannetier, S., Zackai, E., Young, I., Mandel, J.L., Sassone-Corsi, P., and Hanauer, A. (1996). Mutations in the kinase Rsk-2 associated with Coffin-Lowry syndrome. Nature *384*, 567–570.

Wisden, W., and Morris, B.J. (1994). In situ hybridization with synthetic oligonucleotide probes. In In Situ Hybridization Protocols for the Brain, W. Wisden and B.J. Morris, eds (San Diego, CA: Academic Press), pp. 9–30.

Yamauchi, T., Oike, Y., Kamon, J., Waki, H., Komeda, K., Tsuchida, A., Date, Y., Li, M.X., Miki, H., Akanuma, Y., et al. (2002). Increased insulin sensitivity despite lipodystrophy in Crebbp heterozygous mice. Nat. Genet. *30*, 221–226.